# A NUMERICAL SOLUTION ALGORITHM FOR THE SPATIALLY INHOMOGENEOUS EQUATIONS OF KINETIC BREAKDOWN

M. V. Bochkov and B. N. Chetverushkin

UDC 519.63

A computational algorithm is described, based on the total approximation method. The discussion is centered on the example of the model problem of laser breakdown of high-pressure atomic nitrogen near a metallic surface.

A whole range of processes, referring to various fields of study, such as breakdown in gases, the etching problem in lithography, effects in the ionosphere [1-6], and others, can be described during mathematical simulation by means of the system of equations

$$\frac{\partial \mathbf{v}}{\partial t} + L\mathbf{v} = \mathbf{f}(x, t, \mathbf{v}). \tag{1}$$

Here L is a differential operator (acting on v(x, t) as a function of x), describing several spatially inhomogeneous processes: gasdynamic motion, diffusion, or heat conduction as a function of the type of problem; and the functions f(x, t, v) describe processes of nonequilibrium kinetics, usually related to particle generation and recombination in various physicochemical reactions.

In the present study we use the example of a model problem of low-threshold breakdown of atomic nitrogen by laser irradiation to propose an approach to the solution of the system of equations (1), based on using the total approximation method [7]. In this case the solution of the system of equations (1) is decomposed into two phases:

$$\frac{d\mathbf{v}}{dt} = \mathbf{f}(x, t, \mathbf{v}), \tag{2}$$

$$\frac{\partial \mathbf{v}}{\partial t} + L\mathbf{v} = 0, \tag{3}$$

in each of which one uses numerical methods, allowing effective solution of the system of equations (2) and (3). The specific shape of the suggested computational algorithm will be demonstrated on the example of the problem considered below.

1. Statement of the Problem. $CO_2$ laser radiation ($\hbar\omega$ = 0.117 eV, $G_0 = 10^7$ W·cm$^{-2}$) is incident from the right on a metallic film (molybdenum), surrounded by dense atomic nitrogen (P = 100 atm, N = $2.5 \cdot 10^{21}$ cm$^{-3}$). The cold gas is transparent to radiation, and the flux passes through it to the target surface; in this case part of it is absorbed, and part is reflected in the opposite direction. The surface is heated and starts emitting electrons into the gas, with the electrons then gathering energy as a result of retarding absorption in the field of ions and neutral atoms.

Nitrogen is considered as a two-level monatomic gas,* which can be found in one of three states: ground, excited, and singly ionized state. Each of the states is characterized by

*The given statement of the model problem does not take into account the molecular structure of nitrogen. However, in the authors' opinion the use of this statement in the given study is justified for two reasons. Firstly, as shown for the case of nitrogen breakdown by emission of a neodymium laser [8], account of the molecular structure provides only a quantitative variation, without changing the qualitative nature of the process flows. Secondly, the shape of the gas structure used is nowhere reflected in the computational algorithm. Therefore, its description is naturally carried out on the simplest case example of atomic nitrogen.

M. V. Keldysh Institute of Applied Mathematics, Academy of Sciences of the USSR, Moscow.
Translated from Inzhenerno-Fizicheskii Zhurnal, Vol. 55, No. 4, pp. 629-638, October, 1988. Original article submitted June 24, 1987.


0022-0841/88/5504-1154$12.50 

the level population. The following elementary processes are taken into account by means of the rate coefficients of the corresponding reactions: excitation and de-excitation of an atom, ionization by electron impact from the ground and excited state, and three-particle recombination. The electron temperature in the emission zone is caused by elastic, inelastic, and superelastic collisions with heavy particles; the electron thermal conductivity is also taken into account. Since energy exchange between the electron gas and heavy particles is rendered difficult, the problem is considered in the two-temperature approximation.

The processes occurring in the emission band are characterized by strong spatial inhomogeneity, therefore an important role is played by ion and electron diffusion, and the electric currents due to uncompensated charge of thermoelectrons. In the mathematical model we also took into account intensity enhancement of laser radiation due to its partial reflection from the surface and the decrease in flow intensity at the later breakdown phases, when screening of the target starts. The system of equations [which is a special case of system (1)], describing the kinetics of collisions, energy exchange, and the transport processes, is the following:

$$\frac{dN}{dt} = -(k^+N - \beta^+N^+N_e)N_e - (k^*N - \beta^*N^*)N_e, \tag{4}$$

$$\frac{dN^*}{dt} = (k^*N - \beta^*N^*)N_e - (k^{*+}N^* - \beta^+N^+N_e)N_e, \tag{5}$$

$$\frac{\partial N^+}{\partial t} = (k^+N - \beta^+N^+N_e)N_e + (k^{*+}N^* - \beta^+N^+N_e)N_e + \frac{\partial}{\partial x}\left(D^+\frac{\partial N^+}{\partial x}\right) + \frac{\partial}{\partial x}\left(\frac{eD^+}{T_g}N^+\frac{\partial u}{\partial x}\right), \tag{6}$$

$$\frac{\partial N_e}{\partial t} = (k^+N - \beta^+N^+N_e)N_e + (k^{*+}N^* - \beta^+N^+N_e)N_e + \frac{\partial}{\partial x}\left(D_e\frac{\partial N_e}{\partial x}\right) - \frac{\partial}{\partial x}\left(\frac{eD_e}{T_e}N_e\frac{\partial u}{\partial x}\right), \tag{7}$$

$$\frac{3}{2}N_e\frac{\partial T_e}{\partial t} = \mu G - \left(I^* + \frac{3}{2}T_e\right)(k^*N - \beta^*N^*)N_e - \left(I^+ + \frac{3}{2}T_e\right)(k^+N - \beta^+N^+N_e)N_e - \left(I^{*+} + \frac{3}{2}T_e\right)(k^{*+}N^* -$$

$$- \beta^+N^+N_e)N_e - \frac{3m_e}{m_g}(T_e - T_g)\nu N_e + \frac{\partial}{\partial x}\left(\varkappa\frac{\partial T_e}{\partial x}\right), \tag{8}$$

$$\frac{3}{2}N_g\frac{dT_g}{dt} = \frac{3m_e}{m_g}(T_e - T_g)\nu N_e, \tag{9}$$

$$\frac{d^2u}{dx^2} = 4\pi e(N_e - N^+). \tag{10}$$

Expression (4) is a balance equation for ground-state level populations, and Eqs. (5)-(9) are the balance equations for the excited level, for ions, for electrons, the energies for electrons and for heavy particles, respectively, while expression (10) is the one-dimensional Poisson equation.

The values of coefficients and constants appearing as parameters in the equations of system (4)-(10) were used in the same way as in the numerical simulation of low-threshold breakdown by neodymium laser radiation [1, 2, 8]. For the absorption coefficient $\mu$, we used the expression for a monochromatic plane wave propagating in a weakly ionized gas:

$$\mu = \frac{4\pi e^2\nu N_e}{m_e c(\omega^2 + \nu^2)}, \quad \nu = \nu_{ea} + \nu_{ei},$$

$$G = G_0\left[\exp\left(-\int_x^l \mu dx\right) + (1 - A)\exp\left(-\int_x^l \mu dx - \int_0^x \mu dx\right)\right], \quad A = 0{,}2.$$

The classical approximation is valid for $CO_2$-laser [9], since its energy quantum ($\hbar\omega$ = 0.117 eV) is smaller by orders of magnitude than electron temperatures characteristic of laser breakdown. It must be noted that the absorption coefficient value of molybdenum A for a $CO_2$-laser is strongly enhanced.

The boundary conditions for the equations

$$\frac{\partial N^+}{\partial t}=\frac{\partial}{\partial x}\left(D^+\frac{\partial N^+}{\partial x}\right);\quad \frac{\partial N_e}{\partial t}=\frac{\partial}{\partial x}\left(D_e\frac{\partial N_e}{\partial x}\right); \tag{11}$$

$$\frac{3}{2}N_e\frac{\partial T_e}{\partial t}=\frac{\partial}{\partial x}\left(\varkappa\frac{\partial T_e}{\partial x}\right);\quad \frac{d^2u}{dx^2}=4\pi e(N_e-N^+) \tag{12}$$

were given in the form

$$D_e\frac{\partial N_e}{\partial x}\Big|_{x=0}=-\frac{B}{e}T_0^2\exp\left(-\frac{\varphi}{T_0}\right);\quad N^+|_{x=0}=N^+|_{x=l}=N_e|_{x=l}=0; \tag{13}$$

$$T_e|_{x=0}=T_0=\frac{2A}{\lambda}\sqrt{\frac{at}{\pi}}G|_{x=0};\quad \frac{\partial T_e}{\partial x}\Big|_{x=l}=0;\quad u|_{x=0}=u|_{x=l}=0 \tag{14}$$

at the point x = 0 (on the surface) and at the point x = ℓ, located quite far to the right of the film (ℓ = 1 cm).

The Richardson equation [10] was used to estimate the thermoelectron current from a single target surface. The surface temperature was determined by solving the heat conduction problem for a semiinfinite body, acted upon by a constant intensity source. The boundary conditions for the Poisson equation were assigned with account of the fact that no external forces act on the system. A more detailed physical statement of the problem was described in [11].

2. Computational Algorithm. A difference grid was used, being nonuniform in space and in time. The value of the spatial step was assigned in the form of a geometric progression with quotient q (q = 1.22)

$$\omega_{h\tau}=\Big\{(x_i,\ t_j);\ x_i=\frac{q^i-1}{q^{M+1}-1}l,\ 0\leqslant i\leqslant M+1=50;\ t_{j+1}=t_j+\tau_j,$$

$$j=0,\ 1,\ 2\ \ldots\Big\}.$$

In this case the coordinate of the first spatial point away from the surface is $x_1\approx 10^{-5}$ cm. The value of the step in time $\tau_j$ for each time layer was selected directly during the calculation.

A universal method for reducing the complex and awkward mathematical problem to a difference scheme is the total approximation method [7], whose basic idea is that the process of searching an approximate solution consists of a succession of steps, in each of which a simpler problem is solved. In the given case, according to the total approximation method the system of equations (4)-(10) at each step in time $\tau_j$ is represented in the form of two successively solvable systems similar to (2) and (3):

$$\frac{dN}{dt}=-(k^+N-\beta^+N^+N_e)N_e-(k^*N-\beta^*N^*)N_e, \tag{15}$$

$$\frac{dN^*}{dt}=(k^*N-\beta^*N^*)N_e-(k^{*+}N^*-\beta^+N^+N_e)N_e, \tag{16}$$

$$\frac{dN^+}{dt}=(k^+N-\beta^+N^+N_e)N_e+(k^{*+}N^*-\beta^+N^+N_e)N_e, \tag{17}$$

$$\frac{dN_e}{dt}=(k^+N-\beta^+N^+N_e)N_e+(k^{*+}N^*-\beta^+N^+N_e)N_e, \tag{18}$$

$$\frac{3}{2}N_e\frac{dT_e}{dt}=\mu G-\frac{3m_e}{m_g}(T_e-T_g)\nu N_e-\Big[\left(I^*+\frac{3}{2}T_e\right)(k^*N-\beta^*N^*)+$$

$$+\left(I^++\frac{3}{2}T_e\right)(k^+N-\beta^+N^+N_e)+\left(I^{*+}+\frac{3}{2}T_e\right)(k^{*+}N^*-\beta^+N^+N_e)\Big]N_e, \tag{19}$$

$$N_g \frac{dT_g}{dt} = \frac{2m_e}{m_g}(T_e - T_g)\nu N_e; \tag{20}$$

$$\frac{\partial N^+}{\partial t} = \frac{\partial}{\partial x}\left(D^+ \frac{\partial N^+}{\partial x}\right) + \frac{\partial}{\partial x}\left(\frac{eD^+}{T_g} N^+ \frac{\partial u}{\partial x}\right), \tag{21}$$

$$\frac{\partial N_e}{\partial t} = \frac{\partial}{\partial x}\left(D_e \frac{\partial N_e}{\partial x}\right) - \frac{\partial}{\partial x}\left(\frac{eD_e}{T_e} N_e \frac{\partial u}{\partial x}\right), \tag{22}$$

$$\frac{3}{2} N_e \frac{\partial T_e}{\partial t} = \frac{\partial}{\partial x}\left(\varkappa \frac{\partial T_e}{\partial x}\right), \tag{23}$$

$$\frac{d^2u}{dx^2} = 4\pi e(N_e - N^+). \tag{24}$$

The transition from time layer j to (j + 1) is realized in such a manner that initially one solves on the segment $[t_j, t_{j+1}]$ the system of kinetic equations (15)-(20), and then, using the values obtained as initial data for the same step in time one solves the system of diffusion and heat-conduction equations (21)-(23), since the equations of system (15)-(20) are independent of the explicit form of the electric potential u.

The general difference scheme consists of a chain of two difference schemes. The basic meaning of applying the total approximation method in the form (15)-(20), (21)-(23) consists of the fact that at each of its phases, instead of a system of partial differential equations one obtains a system of ordinary differential equations (ODE), for whose solution one can use highly effective multistep numerical methods, including rigorously stable ones. At various spatial points the system of ODEs (15)-(20) was solved separately (independently). In this case the first stage of the total approximation method reduces to that at each point $x_i$ (besides the boundary points i = 0, i = M + 1) one integrates the system of ODEs (15)-(20) from the point $t = t_j$ to the point $t = t_{j+1}$, i.e., one solves for it on the segment $[t_j, t_{j+1}]$ the Cauchy problem, using as initial data the values obtained in solving the system of equations (21)-(24). To integrate the ODE systems we used a standard program, realizing a numerical method of the predictor-corrector type with automatic selection of the step and order of the method. Since this program selects the integration step, starting from assigning its accuracy, then in solving the system (15)-(20) at the segment $[t_j, t_{j+1}]$ one carried out not one step in time, but several or even many. The number of these steps at various points $x_i$ was different, since the variation occurred substantially nonuniformly in space. Usually there were from 4-5 to 20-30 steps in time in the segment $[t_j, t_{j+1}]$.

Thus, in solving the system (15)-(20), at each point $x_i$ we used its difference grid in time, being smaller than $\omega_{h\tau}$. A detailed approach is useful when nonequilibrium kinetic processes occur differently at various spatial points. The specifics of the program with automatic selection of the step and the order of the method consist of that the initial step is usually relatively small, and then, with further integration the step used usually increases substantially, sometimes by several orders. Since the application of multistep high-order approximation methods to the system of ODEs (15)-(20) allowed to integrate it with a crude step in time, in several cases it was suitable to strongly enhance the length of the segment $[t_j, t_{j+1}]$, so that it exceeded the time step with which the system of equations (21)-(24) could be solved. Consequently, to enhance the effectiveness of the algorithm in several cases, and in solving the system of equations (21)-(24) on the segment $[t_j, t_{j+1}]$ several steps in time (usually 5-10) were made.

For the system of ODEs (15)-(20) to be solved at the time step $[t_j, t_{j+1}]$ corresponding to the point $x_i$ independently of other spatial points it is necessary to assume that

$$G(x_i, t) = \text{const} \quad \text{for} \quad t_j < t < t_{j+1}. \tag{25}$$

In the problem solved, due to the fact that the laser radiation flux varies weakly with time, it appeared possible to simply select it with the preceding layer: $G(x_i, t) = G(x_i, t_j)$ for $t_j < t < t_{j+1}$.

The computational algorithm was suggested in [11]-[13]. It is an updated algorithm, used in [1, 2] for numerical solution of a system of equations similar to (1)-(7). In [1, 2] the total approximation method was also used in the form of decomposing the original system into two subsystems, so as to decouple the system of inhomogeneous partial differential

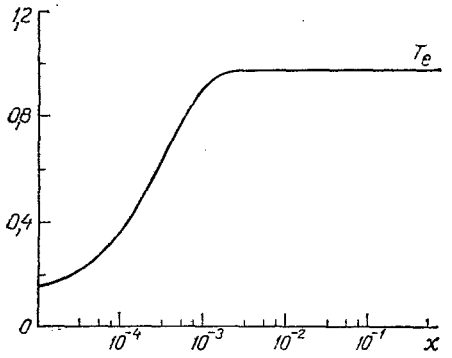


Fig. 1

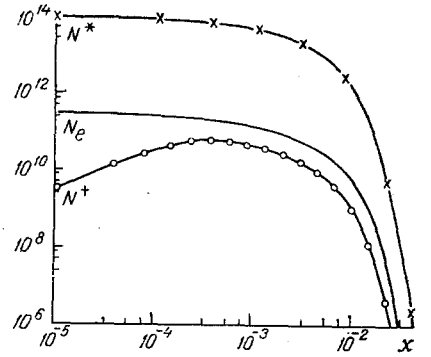


Fig. 2

Fig. 1. Spatial profile of the electron temperature at the moment of time $t = 2 \cdot 10^{-10}$ sec; x in cm, $T_e$ in eV.

Fig. 2. Spatial concentration profiles at the moment of time t = 2 μsec. $N^*$, $N^+$, $N_e$ in $cm^{-3}$.

equations into a system of homogeneous partial differential equations and a system of ODEs. However, no assumptions similar to (25) were made in [1, 2], and the ODE system obtained was solved simultaneously at all spatial points, quite similarly to the way it was done in the direct method [4]. According to the method of [1, 2], the first phase of the total approximation method consists of integrating on the segment $[t_j, t_{j+1}]$ one large system of ODEs containing 6M equations. We recall that in the present study the first phase of the total approximation method was reduced to the necessity of solving on the segment $[t_j, t_{j+1}]$ M ODE systems, each of which containing six equations. Practice shows that the computational algorithm in its present form decreases by many times the required computer memory and computational time of a single variant.

Obviously, one can isolate two basic factors, capable of substantially reducing the computational time in the transition from simultaneous solution of the system (15)-(20) at all spatial points to its separate point-by-point solution. One of these factors is that the large system, combining the equations for all spatial points, can be more difficult than each of the small systems separately. This can occur, for example, if there exists a substantial spatial inhomogeneity of physical processes. The program integrating the ODE system selects by itself the time step, starting from its assigned accuracy. For single spatial points this step can be substantially smaller than for others. The use of the general (large) system of equations induces at all spatial points integration with one and the same time step, which at each given moment is limited by an "unpleasant" spatial point.

Another factor is that for most algorithms of integrating ODE systems the number of arithmetic operations is proportional to the square of the number of equations (usually this is related to the necessity of inverting Jacobi matrices). For most ODE systems containing 6M equations the number of arithmetic operations is of order $(6M)^2$. At the same time, if it is necessary to solve M systems of six equations each, the number of arithmetic operations is of order $6^2M$. Due to the fact that the Jacobi matrix of the total system of equations contains a larger number of equations than the total number of elements in the small Jacobi matrices, in the separate solution of small systems one obtains a gain in computational time.

3. Several Results of Numerical Calculations. The results of solving the model problem described above are shown in Figs. 1-4. In each of the figures are shown spatial profiles of the variables at various moments of time; in this case it is assumed that the laser radiation starts acting at t = 0.

Directly following the laser action there starts rapid growth of the electron temperature $T_e$, and following time $t \approx 2 \cdot 10^{-10}$ sec it reaches a stationary value (Fig. 1). The value of the established electron temperature ($T_e = 0.98$ eV for $x \geq 3 \cdot 10^{-4}$ cm) is independent of the concentration $N_e$ and is mostly determined by the relation between the values of P and G, therefore in what follows, during the duration of the whole process the electron temperature is practically unchanged up to the origin of the screening surface.

The metallic surface is heated relatively slowly, and to this is related the basic delay in the development of an electron avalanche. To the extent of growth of surface temperature

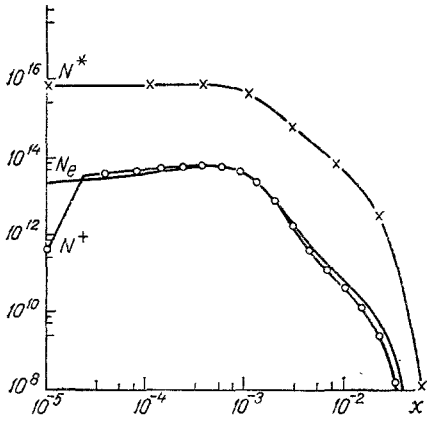


Fig. 3

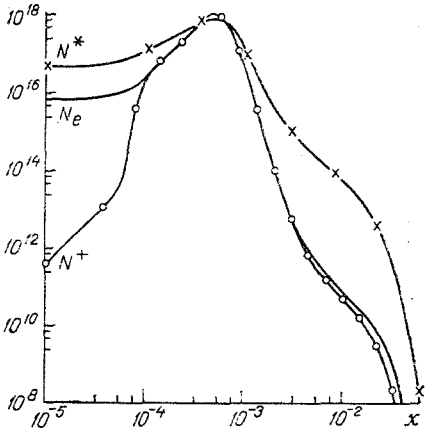


Fig. 4

Fig. 3. Spatial concentration profiles at the moment of time t = 3.5 μsec.

Fig. 4. Spatial concentration profiles at the moment of time t = 3.605 μsec.

($T_0 \sim AG_0\sqrt{t}$), the thermoemission current from the metal to the gas medium (Fig. 2) starts being enhanced. The high pressure of nitrogen hinders electron drift at large distances from the film, and therefore their concentration at the surface increases. The contribution of ionization to increasing $N_e$ at this phase of the process is negligibly small ($N_e \gg N^+$).

As seen from the figure, the enhancement in electron concentration in the near-surface layer leads to noticeable growth in the number of excited atoms. This has a large value, since in the following a basic role is played by the mechanism of power-law ionization. To the extent of increased effect of ionization processes one observes a gradual approach of the ionic concentration to that of the electrons (Fig. 3). The equality $N_e \approx N^+$ implies that thermoemission is not a large basic source of enhanced $N_e$. This is also indicated by the variation in the electron concentration profile, i.e., by the appearance of a maximum in the region $x \approx 5 \cdot 10^{-4}$ cm (Figs. 3, 4). Now the electrons, created in ionization acts in the gas volume, diffuse to the surface of the target.

At the concluding phase of breakdown ionization prevails not only over thermoemission, but also over atomic excitation, while one observes a sharp increase in the rate of evolution of electron avalanche. As shown from Fig. 4, breakdown occurs in a very narrow region, practically on the metallic surface. At moment of time $t \approx 3.605$ μsec there occurs substantial screening of the target surface. This leads to lowering of the electron gas temperature $T_e$. The energy of laser radiation absorbed in the breakdown zone reaches several percent of its total flux, therefore the process of primary breakdown of cold nitrogen can be assumed to be completed. In what follows the breakdown zone starts being shifted to the right, toward the laser emission.

The intensely absorbing plasma layer formed near the surface quickly leads to its total screening, and thus leads to vanishing reflected flux of laser radiation. Therefore the electron temperature $T_e$, which was primarily determined by the sum of incident and reflected fluxes, is substantially diminished not only inside the absorbing zone, but also in the region of the transparent gas. If the intensity $G_0$ is near the threshold, breakdown can be further damped.

The maximum breakdown surface temperature reached in the breakdown process $T_0 = 2290°C$ (for t = 3.6 μsec) is less than even the melting temperature of molybdenum at atmospheric pressure: $T_{melt} = 2620°C$. This, obviously, justifies the model assumption concerning the absence of material evaporation near the target.

In conclusion, it is noted once more that the algorithm suggested, based on the use of the total approximation method, is sufficiently general for modeling effects in which a substantial role is played by nonequilibrium kinetic processes. Finally, depending on the specific problem the numerical methods used for solving the system (2) and (3) may vary. However, the use of the principle itself of partitioning the original problem, so that at one

of the phases of the total approximation method the system of partial differential equations is replaced by a system of ODEs, is effective for the solution of a wide class of problems.

## NOTATION

$N$, $N^*$, $N^+$, $N_e$, $N_g$, concentrations of nonexcited atoms, excited atoms, ions, electrons, and heavy particles; $T_e$, $T_g$, temperatures of electrons and heavy particles; $u$, electric potential; $t$, time; $x$, spatial coordinate; $I^*$, $I^+$, $I^{*+}$, excitation and ionization energies of atoms from the ground and excited states; $k^*$, $k^+$, $k^{*+}$, rate coefficients of excitation and ionization; $\beta^*$, $\beta^+$, rate coefficients of deexcitation and recombination; $\mu$, absorption coefficient of radiation; $\nu_{ei}$, $\nu_{ea}$, frequencies of elastic electron collisions with ions and atoms; $D^+$, $D_e$, diffusion coefficients of ions and electrons; $\kappa$, electron heat conduction coefficient; $G_0$, inlet power flux of laser radiation; $G$, actual power flux of radiation at the point $x$; $e$, $m_e$, $m_g$, electron charge and mass, and atomic mass; $B$, thermoemission constant; $\varphi$, work function; $T_0$, surface temperature; $\lambda$, $a$, thermal conductivity and thermal diffusivity coefficients of molybdenum; $A$, absorption coefficient of radiation by a plate; $\omega$, frequency of laser radiation; $c$, velocity of light; $\hbar$, Planck constant; $P$, pressure of nitrogen; $\ell$, length of the integration segment; $\omega_{h\tau}$, difference network; $q$, ratio of the geometric progression; $x_i$, $t_j$, $t_{j+1}$, i-th site of the spatial network, and the j-th and (j + 1)-th sites of the time network; $\tau_j$, j-th step in time; and $M$, number of internal sites of the spatial network.

## LITERATURE CITED


1. V. I. Mazhukin, A. A. Uglov, and B. N. Chetverushkin, Dokl. Akad. Nauk SSSR, 246, No. 6, 1338-1342 (1979).
2. V. I. Mazhukin, A. A. Uglov, and B. N. Chetverushkin, Zh. Vychisl. Mat. Mat. Fiz., 20, No. 2, 451-460 (1980).
3. K. A. Valiev and T. M. Makhviladze, Poverkhnost', No. 3, 57-67 (1985).
4. K. A. Valiev, T. M. Makhviladze, and M. E. Sarychev, Dokl. Akad. Nauk SSSR, 283, No. 2, 366-369 (1985).
5. G. V. Khazanov, M. A. Koen, Yu. V. Konikov, and I. M. Sidorov, Planet. Space Sci., 32, No. 5, 585-598 (1984).
6. L. V. Zinin, Yu. I. Galperin, K. S. Latyshev, and S. A. Grigoriev, Results of the ARCAD 3 PROJECT and of the recent programmes in magnetospheric and ionospheric physics (International Conference, Toulouse, May 22-25, 1984), Toulouse (1985), pp. 391-408.
7. A. A. Samarskii, Theory of Difference Schemes [in Russian], Moscow (1983).
8. V. I. Mazhukin, A. A. Uglov, and B. N. Chetverushkin, Kvantovaya Elektron., 10, No. 4, 679-701 (1983).
9. Yu. P. Raizer, Fundamentals of Contemporary Physics of Gas-Discharge Processes [in Russian], Moscow (1980).
10. K. Shimony, Physical Electronics [Russian translation], Mir (1977).
11. M. V. Bochkov and B. N. Chetverushkin, "An algorithm of numerical solution of the equations of kinetic breakdown," Preprint, Moscow (1985).
12. M. V. Bochkov and B. N. Chetverushkin, "A method of numerical solution of the system of equations of a partially ionized plasma in the model of three-fluid hydrodynamics," Preprint, Moscow (1985).
13. M. V. Bochkov and B. N. Chetverushkin, Proc. All-Union School Young Scientists (Shushenskoe, September 8-15, 1986), Krasnoyarsk (1986), pp. 115-116.
14. S. M. Gol'berg, A. Yu. Zakharov, and S. S. Filippov, "Several numerical solutions of systems of ordinary differential equations," Preprint, Moscow (1976).